Published in final edited form as:
Nat Genet. 2008 August ; 40(8): 963–970. doi:10.1038/ng.188.

Ribosomal mutations cause p53-mediated dark skin and pleiotropic effects

Kelly A McGowan[1], **Jun Z Li**[1,2,7], **Christopher Y Park**[3], **Veronica Beaudry**[4], **Holly K Tabor**[1,2,7], **Amit J Sabnis**[1,7], **Weibin Zhang**[1], **Helmut Fuchs**[5], **Martin Hrabé de Angelis**[5], **Richard M Myers**[1,2,7], **Laura D Attardi**[1,4], and **Gregory S Barsh**[1,6]

[1]Department of Genetics, Stanford University, Stanford, California 94305, USA.

[2]Stanford Human Genome Center, Stanford University, Stanford, California 94305, USA.

[3]Department of Pathology, Stanford University, Stanford, California 94305, USA.

[4]Department of Radiation Oncology, Division of Radiation and Cancer Biology, Stanford University, Stanford, California 94305, USA.

[5]Helmholtz Zentrum Muenchen, German Research Center for Environmental Health, Institute of Experimental Genetics, Neuherberg D-85764, Germany.

[6]Department of Pediatrics, Stanford University, Stanford, California 94305, USA.

Abstract

Mutations in genes encoding ribosomal proteins cause the Minute phenotype in *Drosophila* and mice, and Diamond-Blackfan syndrome in humans. Here we report two mouse dark skin (*Dsk*) loci caused by mutations in *Rps19* (ribosomal protein S19) and *Rps20* (ribosomal protein S20). We identify a common pathophysiologic program in which p53 stabilization stimulates Kit ligand expression, and, consequently, epidermal melanocytosis via a paracrine mechanism. Accumulation of p53 also causes reduced body size and erythrocyte count. These results provide a mechanistic explanation for the diverse collection of phenotypes that accompany reduced dosage of genes encoding ribosomal proteins, and have implications for understanding normal human variation and human disease.

Mutants with the dominantly inherited Minute phenotype, first described in flies more than 85 years ago, share common features, including delayed larval development, abnormal bristles and recessive lethality[1]. Because of these phenotypic similarities, it is not surprising that Minute loci encode genes in a common pathway: thus far, all known mutations affect ribosomal proteins, in both the 40S (encoded by *Rps* genes) and 60S (encoded by the *Rpl* genes) subunits[2]. *Rps* and *Rpl* mutations have also been described in other species, including mice and humans[3,4]. *RPS19* and, more recently, *RPS17* and *RPS24* sequence alterations have been identified in individuals with Diamond-Blackfan syndrome, in which congenital red blood cell aplasia is associated with growth retardation and limb and/or craniofacial

Correspondence should be addressed to G.S.B. (gbarsh@stanford.edu)..
[7]Present addresses: Department of Human Genetics, School of Medicine, University of Michigan, Ann Arbor, Michigan 48109, USA (J.Z.L.), Center for Biomedical Ethics, Stanford University, Stanford, California 94305, USA (H.K.T.), University of California, San Francisco, School of Medicine, San Francisco, California 94143, USA (A.J.S.) and HudsonAlpha Institute for Biotechnology, Huntsville, Alabama 35486, USA (R.M.M.).

Supplementary information is available on the Nature Genetics website.

Accession codes. NCBI GEO: gene expression data have been deposited with accession code GSE11331. GenBank: *Impad1*, NM_177730; *Rps20*, NM_026147.

malformations[4–7]. In most affected individuals, *RPS* mutations are heterozygous and sporadic; inherited forms of familial Diamond-Blackfan syndrome also exist in which *RPS* mutations segregate in an autosomal dominant manner[7–9]. Akin to Minute flies, the genotype–phenotype association between *RPS* mutations and the human disorder is strong, yet the molecular mechanisms underlying the specific phenotypes observed in humans remain enigmatic.

Studies in unicellular organisms and cultured mammalian cells have shown that *Rps* and *Rpl* mutations compromise ribosome biogenesis and protein synthesis[3,10–12]. In addition, mutant cells show decreased rates of proliferation and a survival disadvantage in mosaic and chimeric animals[3,11,13]. Although some phenotypes may be the direct result of abnormal cell cycle kinetics, it is not known how mutations that impair protein synthesis and cell cycle dynamics yield tissue-specific phenotypes such as anemia.

During the course of a forward genetic screen in mice for pigmentary abnormalities, we identified missense alterations of *Rps19* and *Rps20* in two mutants with dominantly inherited dark skin, *Dark skin 3* (*Dsk3*) and *Dark skin 4* (*Dsk4*), respectively. Using a combination of cell biological and genetic approaches, we show that abnormalities caused by mutations in genes encoding ribosomal proteins are mediated by a common pathophysiologic mechanism that involves activation and/or stabilization of p53. Often referred to as the guardian of the genome because its activation in response to genomic stress helps to prevent cancer, p53 also contributes to the pathogenesis of several human diseases when activated[14]. Here we show that the ‘dark side’ of p53 is pleiotropic, with distinct phenotypic outcomes that depend on the underlying cell type in which activation occurs, providing new insight into pigmentary biology, erythrocyte development and human disease.

RESULTS

Epidermal melanocytosis in *Dsk* mutants

Dsk3 and *Dsk4* were identified in a large-scale chemical mutagenesis screen for dominant traits affecting morphology, blood chemistry or behavior[15]. From approximately 32,000 animals, 15 Dsk mutants were recovered that represent three phenotypic categories: adult-onset dark skin associated with epidermal thickening, accumulation of dermal melanocytes during development and accumulation of epidermal melanocytes during development[16]. We have previously described molecular defects responsible for the first two categories[16,17]; *Dsk3* and *Dsk4* represent the third category.

Increased pigmentation in *Dsk3* and *Dsk4* becomes apparent by 3 weeks of age in the footpad, tail and ears of mutant animals and persists throughout adult life (**Fig. 1a** and data not shown). Using a quantitative assay for the degree of pigmentation in separate layers of tail skin, we found that pigment accumulates in the mutant epidermis compared to the nonmutant epidermis, whereas the dermis is unaffected (**Fig. 1b,c**). This conclusion was confirmed by histological analysis showing excess pigment in the epidermis of *Dsk3* and *Dsk4* footpads, tail and ear (**Fig. 1d** and data not shown).

We used a histochemical marker for pigment cells, a *lacZ* transgene driven by regulatory elements from the *Dct* (dopachrome tautomerase) gene[18], to determine whether excess epidermal pigmentation is caused by an increased number of melanocytes or by increased melanin production. We found that *Dsk3* and *Dsk4* footpad epidermis is characterized by an increased number of Xgal-positive cells located in the basal layer (**Fig. 1e–g**). Excess cells are first apparent in the mutant footpad at postnatal day 3 (P3), and persist in the adult footpad (**Supplementary Fig. 1a** online).

We studied the ontogeny of this process by examining midgestation mutant and nonmutant embryos. At embryonic day 10 (E10), the *Dct-lacZ* transgene marks melanoblasts as they leave the neural crest; by E15, pigment cell precursors have moved to the developing skin in a dorsal to ventral expansion (**Fig. 1h**)[18–20]. Of note, we found that *Dsk3* and *Dsk4* mutant embryos have fewer Xgal-positive cells than nonmutant animals at all embryonic time points examined (**Fig. 1h, Supplementary Fig. 1b** and data not shown). In fact, a white belly spot, a cutaneous location in which melanocytes fail to populate during development[21,22], was observed in approximately 10% of *Dsk3* adults, and was enhanced when placed on a genetic background sensitized by the presence of the Kit^{Wv} mutation (**Supplementary Fig. 1c**). Thus, epidermal melanocytosis in *Dsk3* and *Dsk4* occurs postnatally. Furthermore, these mutations have opposite effects at different times: during embryogenesis, the *Dsk3* and *Dsk4* mutations impair pigment cell development, but after birth, they cause pigment cells to accumulate progressively in the adult epidermis.

Positional cloning of *Dsk3* and *Dsk4*

Dsk3 and *Dsk4* were initially localized to 4.49- and 3.85-cM intervals on chromosomes 7 and 4, respectively[16]. By generating and evaluating ~1,500 additional backcross progeny, we narrowed these intervals to 0.6 and 4.7 Mb, respectively (**Fig. 2a** and **Supplementary Fig. 2a** online), within which no known pigmentation genes were apparent. Despite its smaller size, the *Dsk3* critical interval is very gene-dense compared to that of *Dsk4*; therefore, we focused initially on the latter. We sequenced the exons and proximal 5′ flanking regions of all 19 candidate genes in the critical interval (chr4: 3.6–9.3 Mb, genome assembly mm8) and identified two nucleotide substitutions in *Dsk4*-mutant mice compared to the strain of origin: a point mutation (T2201A) in the 3′ UTR of *Impad1* (inositol monophosphatase domain containing 1; NM_177730), and a point mutation (T209C) that predicts a L32P amino acid substitution in *Rps20* (ribosomal protein S20; NM_026147) (**Fig. 2b**).

We then realized that the *Dsk3* critical interval contained a related gene, *Rps19*, which, like *Rps20*, encodes a protein component of the 40S small ribosomal subunit[23]. Within the protein-coding region of *Rps19*, we identified a point mutation (T316A) that predicts a Y54N amino acid substitution (**Supplementary Fig. 2b**).

The aforementioned three mutations were the only sequence alterations identified in a total of approximately 125 kb of sequence, and the predicted amino acid substitutions in Rps19 and Rps20 occur in residues that are evolutionarily conserved among their respective orthologs in unicellular and multicellular organisms (**Fig. 2c,d**). Besides the pigmentary phenotype observed in heterozygous animals, homozygosity for *Dsk3* or *Dsk4* causes early (before E7.5) embryonic lethality (data not shown), a phenotype shared by other ribosomal protein mutants[2,3]. Taken together with the data described below for a third ribosomal protein gene, we conclude that *Dsk3* and *Dsk4* are caused by loss-of-function alterations in *Rps19* and *Rps20*, respectively.

Dark skin is keratinocyte autonomous

To further investigate the effect of ribosomal 40S alterations on pigmentation, and to determine in which cell type those alterations act to cause dark skin, we made use of a conditional knockout allele[11] for a third ribosomal protein subunit gene, $Rps6^{lox}$. Animals homozygous for $Rps6^{lox}$ were crossed to those carrying either a Cre driver expressed in keratinocytes (*Tg.K5Cre*)[24] or in melanocytes (*Tg.MitfCre*)[25] (**Fig. 3a**).

We found that animals with keratinocyte-specific hemizygosity for *Rps6* ($Rps6^{lox/+}$; *Tg.K5Cre*/+) show markedly darkened footpads, ears, tail and hair compared to control

animals (**Fig. 3b,c**). Examination of tail skin showed that pigment accumulates in the epidermis, whereas the dermis is unaffected (**Fig. 3d,e**), a phenocopy of *Rps19*^{Dsk3} and *Rps20*^{Dsk4}. Thus, mutations affecting three different components of the 40S ribosome give rise to similar pigmentary phenotypes, and for at least one of those components, action in keratinocytes is sufficient to cause the mutant phenotype.

By contrast, melanocyte-specific hemizygosity for *Rps6* (in *Rps6*$^{lox/+}$;*Tg.MitfCre*/+ animals) causes lighter skin (**Fig. 3b,d,e**) and affects both the epidermis and, to a lesser degree, the dermis (**Fig. 3d,e**). This phenotype is consistent with a reduction in the number and/or proliferative capacity of melanoblasts, as occurs in animals with impaired Kit signaling, and as we observed in *Rps19*^{Dsk3} and *Rps20*^{Dsk4} mutant embryos (**Supplementary Fig. 1b**)[21,22]. Taken together, these results suggest that the pigmentary phenotypes of the original mutants represent the combination of two opposing processes: mutations of *Rps19* or *Rps20* in melanocytes decrease skin pigmentation, whereas the same mutations in keratinocytes increase skin pigmentation. Consistent with this idea, keratinocyte-specific hemizygosity for *Rps6* causes much darker skin than observed in *Rps19*^{Dsk3} or *Rps20*^{Dsk4} mutant animals (**Figs. 1** and **3**).

Requirement for Kit signaling

Keratinocytes produce a number of paracrine factors that affect pigment cell development, proliferation and behavior, and whose altered expression might cause epidermal melanocytosis[26]. We used quantitative RT-PCR to measure levels of *Kitl* (Kit ligand), *Pomc* (proopiomelanocortin) and *Edn1* (endothelin-1) in mRNA from footpad epidermis of mutant (*Rps6*$^{lox/+}$;*Tg.K5Cre*/+) and nonmutant (*Rps6*$^{lox/+}$) littermates. *Pomc* and *Edn1* mRNA levels were unchanged (**Supplementary Fig. 3a,b** online); however, *Kitl* mRNA levels were elevated 8.2- and 3.8-fold at P3 and P30, respectively, in mutant compared to nonmutant animals (**Fig. 4a**). We also found *Kitl* to be expressed at higher levels in the footpad epidermis of *Rps19*$^{Dsk3/+}$ and *Rps20*$^{Dsk4/+}$ compared to nonmutant animals (**Fig. 4b,c**).

A previous study[27] using a *Kitl* transgene driven by a keratinocyte promoter indicated that high expression of *Kitl* gives rise to epidermal melanocytosis, similar to, albeit more severe than, the dark skin in our *Rps* mutants. To investigate a potential requirement for Kit signaling in the *Rps* dark skin mutants, we made use of a neutralizing antibody for Kit, Ack2 (ref. 28). Homozygotes for the *Rps6*^{lox} allele were crossed to animals carrying *Tg.K5Cre*, and mutant (*Rps6*$^{lox/+}$;*Tg.K5Cre*/+) and nonmutant (*Rps6*$^{lox/+}$) littermates were injected at P2 with either Ack2 antisera or phosphate-buffered saline (PBS). In footpads examined at P8, we observed that PBS injection had no effect on pigmentation in either mutant or nonmutant animals, but that Ack2 injection prevented dark skin in the mutant animals (**Fig. 4d**). These results demonstrate that Kit signaling is required for dark skin caused by *Rps* mutations, and suggest that the elevated levels of *Kitl* mRNA have a critical role in that process.

Gene expression signatures for melanocytes and p53

To explore whether increased expression of *Kitl* was part of a larger transcriptional program caused by reduced *Rps* gene dosage, we used whole-genome microarrays to measure gene expression in mRNA from P3 footpad epidermis. We prepared RNA for each hybridization from the epidermis of four rear footpads (two animals) and carried out three biological replicates for mutant (*Rps6*$^{lox/+}$;*Tg.K5Cre*/+) and nonmutant (*Rps6*$^{lox/+}$) epidermis.

We analyzed the microarray data by directly comparing the expression for each gene in mutant compared to nonmutant, and identifying genes whose expression between the two groups seemed significantly different. A global view of these results (**Fig. 4e**) revealed that

the effects of reduced *Rps6* gene dosage are subtle: only 25 of the 24,611 transcripts (~0.1%) represented on the array were associated with *P* values <0.05 (Benjamini-Hochman correction for false-discovery rate)[29]. In addition, most of the changes in the mutant sample represent induction rather than repression (**Fig. 4e**); only 5 of the 25 genes associated with a *P* value <0.5 were repressed (χ^2 test $P = 0.0027$), and the average change as a multiple of control of induced genes was 4.12 compared to 0.82 for repressed genes (**Supplementary Table 1** online). These observations suggest that reduced gene dosage of *Rps6* elicits a specific biological response rather than a global effect on the transcriptome.

Two transcriptional signatures emerge from the microarray data that provide insight into the pathogenesis of dark skin. First, four melanocyte-selective genes, including *Slc45a2* (membrane associated transporter), *Sox10* (SRY-box containing gene 10), *Si* (silver) and *Ednrb* (endothelin receptor type b), seem induced in mutant epidermis; as such, these are likely to reflect an increased number of melanocytes rather than altered transcription *per se* (**Supplementary Table 1**). Second, and more importantly, several genes known to be transcriptional targets of p53 were induced in the mutant tissue, including *Mdm2* (mouse double minute 2), *Ddit4l* (DNA-damage inducible transcript 4-like) (**Supplementary Table 1**)[30,31], and others (L. Attardi, unpublished data).

Dark skin and erythrocyte hypoplasia are mediated by *Trp53*

On the basis of the microarray data, we hypothesized that p53 stabilization and/or activation might be a critical event linking reduced *Rps* gene dosage in keratinocytes to increased expression of *Kitl* and consequent epidermal melanocytosis. This idea is supported by previous studies demonstrating that reduced dosage of *Rps6* in the early mouse embryo[32] or in T lymphocytes[33] triggers apoptosis and cell cycle arrest in a p53-dependent manner.

We first looked for evidence of altered p53 expression by immunohistochemistry of footpad epidermis. From tissues processed in parallel, we observed a 73-fold increase in p53 staining that was strongest in the basal layer of the epidermis in *Rps6*$^{lox/+}$;*Tg.K5Cre* animals compared to nonmutant controls (*Rps6*$^{lox/+}$) (**Fig. 5a** and **Supplementary Fig. 4b,c** online). Similar results were observed in *Rps19*^{Dsk3} and *Rps20*^{Dsk4} animals (**Supplementary Fig. 5a** online). A modest elevation of p53 staining (sevenfold) was also observed in the footpad epidermis of *Tg.K5Cre* heterozygous animals compared to nonmutant animals (an observation that is consistent with the findings of others[34,35]), but it did not affect footpad pigmentation (**Supplementary Fig. 5a–c**).

To investigate a potential role for p53 more critically, we used a previously characterized conditional *Trp53* allele generated by gene targeting embryonic stem cells, *Trp53*$^{LSL\text{-}QS}$, in which expression of a mutant form of p53 (L25Q, W26S) is triggered by Cre recombinase[36]. The p53^{QS} protein is compromised for transactivation but retains biological activity in apoptosis and growth suppression. Importantly, the mutant allele is controlled by endogenous *Trp53* regulatory sequences—levels of *Trp53*^{QS} mRNA are normal (after activation by Cre recombinase)—but the L25Q and W26S substitutions render the protein resistant to the E3 ubiquitin ligase Mdm2, leading to increased levels of p53^{QS} protein.

In animals heterozygous for both *Trp53*$^{LSL\text{-}QS}$ and *Tg.K5Cre* (the latter to activate p53^{QS} in keratinocytes; **Fig. 5b**), we observed markedly darkened footpads, ears, tail and hair (**Fig. 5c** and data not shown). We also found that *Kitl* mRNA expression is increased 5.5-fold in the footpad epidermis of *Trp53*$^{LSL\text{-}QS/+}$; *Tg.K5Cre*/+ compared to control animals (**Fig. 5d**). Thus, activation of p53^{QS} is sufficient to induce increased expression of *Kitl* mRNA and dark skin.

We then asked whether p53 was required for dark skin caused by reduced *Rps* gene dosage. We crossed *Rps6*$^{lox/+}$;*Tg.K5Cre*/+ animals to those carrying a *Trp53* knockout allele[37], *Trp53*^{KO}, and assessed expression of *Kitl* mRNA and skin color. In *Rps6*$^{lox/+}$; *Tg.K5Cre*/+ animals, deficiency for p53 (*Trp53*$^{KO/KO}$) completely reversed the elevation of *Kitl* mRNA and dark skin (**Fig. 5e,f**). In fact, hemizygosity for p53 (*Trp53*$^{KO/+}$) partially ameliorates dark skin; the pigmentary phenotype of *Rps6*$^{lox/+}$; *Tg.K5Cre*/+; *Trp53*$^{KO/+}$ animals is intermediate between that of *Rps6*$^{lox/+}$; *Tg.K5Cre*/+ and *Rps6*$^{lox/+}$;*Tg.K5Cre*/+;*Trp53*$^{KO/KO}$ animals (**Fig. 5e**). A similar effect of the *Trp53*^{KO} allele was observed for *Rps19*^{Dsk3} and *Rps20*^{Dsk4} (**Supplementary Fig. 5b,c**). Thus, p53 is a critical link between reduced *Rps* gene dosage and *Kitl*-induced epidermal melanocytosis.

Finally, the *Rps19*^{Dsk3} allele affords the opportunity to examine the mechanism by which *RPS19* mutations cause abnormalities in humans with Diamond-Blackfan syndrome. Although severely affected individuals have reduced birth weight, limb malformations and complete red cell aplasia, there is both variable expressivity and reduced penetrance; even within families, the same *RPS19* mutation may cause overt Diamond-Blackfan syndrome, isolated macrocytosis and/or elevated erythrocyte adenosine deaminase activity, or be clinically silent[7].

On both the original inbred (C3HeB/HeJ) and a mixed genetic background, we found that *Rps19*^{Dsk3} animals show a lower red blood cell count and growth retardation compared to nonmutant animals; we also observed reduced birth weight (~ 10–15% reduction) and a depressed reticulocyte count (~ 50% reduction) on the inbred background (**Table 1** and **Supplementary Table 2** online). We could not discern any differences in bone marrow cytology between mutant and nonmutant animals (**Fig. 6a**), and the erythrocyte phenotype was mild, with ~ 5% and ~ 10% reductions in red blood cell count at 8 weeks and 20 weeks of age, respectively (**Supplementary Table 3** online). However, as has been described in humans with Diamond-Blackfan anemia[38], we observed increased apoptosis in bone marrow progenitor cells[39] in *Rps19*$^{Dsk3/+}$ compared to nonmutant controls (**Fig. 6b**).

Finally, in a cross with animals carrying the *Trp53*^{KO} allele, we found that reduced dosage of *Trp53* rescued both the erythrocyte and body weight phenotypes caused by *Rps19*^{Dsk3} (**Table 1** and **Supplementary Table 3**). Thus, like dark skin, p53 is a critical and necessary link from reduced *Rps* gene dosage to both tissue-specific (epidermal melanocytosis, erythrocytic hypoplasia) and whole-animal (growth retardation) phenotypes.

DISCUSSION

Although hemizygosity for genes encoding different ribosomal protein subunits has been recognized for decades to cause reduced cellular and organismal growth, *Rps* and *Rpl* mutations have more recently been discovered to cause markedly specific phenotypes, including cancer in zebrafish[40], white spotting in mice[3] and anemia in humans[4–6]. These observations have led to hypotheses for an ‘extraribosomal’ function of certain ribosomal protein subunits, as it is not clear how a general impairment of translation in every cell of the body might have tissue-specific manifestations. Our work demonstrates that mutations of *Rps6*, *Rps19* and *Rps20* each give rise to the same phenotype—dark skin caused by epidermal melanocytosis—and act through a common pathway that depends on accumulation of p53 and increased expression of *Kitl*. These findings demonstrate, on an organismal level, that p53 serves not only as a guardian for DNA damage but also as a sensor of ribosome integrity, provides a mechanistic explanation for both the pleiotropy and tissue specificity that accompany reduced dosage of ribosomal protein genes in many different organisms, and has implications for understanding both normal human variation and human disease.

The connection between epidermal melanocytosis and p53 is surprising, as the typical consequences of p53 activation—apoptosis and cell cycle arrest—might be expected to cause hypo- rather than hyperpigmentation. However, our experiments with the conditional *Rps6* allele indicate that p53 acts in keratinocytes rather than melanocytes to cause dark skin; indeed, our results suggest that p53 activation in developing pigment cells causes the white-spotting phenotype observed in *Dsk3* and *Dsk4* mutants, as would be predicted for cell-autonomous action of p53. It has been demonstrated previously that hemizygosity for *Rps6* causes p53-dependent apoptosis in early mouse development[32] and in adult T cells[33]. Because mutations in *Rps19* and *Rps20* have similar effects, p53 likely plays a general role in sensing ribosome integrity, and may provide a critical link between many ribosomal protein alterations and their phenotypic effects, as in Diamond-Blackfan anemia (see below). We note, however, that the causal link between p53 and *Kitl* in the pathogenesis of dark skin probably does not apply to the erythroid defect, as bone marrow transplantation can cure Diamond-Blackfan anemia[7], but not deficiency for *Kitl*[41]. Thus, the action of Kit ligand on hematopoietic cells is cell non-autonomous, whereas the defect in Diamond-Blackfan anemia is cell-autonomous.

Although the connection between disease phenotypes and p53 generally focuses on loss-of-function mutations, dark skin likely represents a novel endpoint for normal p53 action[14]. From this perspective, we note that Cui *et al*.[42] have also implicated p53 in hyperpigmentation caused by chronic exposure to low levels of UVB irradiation. These investigators postulated that the tanning response is mediated by p53-dependent activation of *Pomc*, thereby promoting changes in pigment synthesis and/or melanocyte differentiation. However, our results suggest that a role for p53 in tanning may also depend on *Kitl*, consistent with the observation of Slominski *et al*.[43] that deficiency of *Pomc* has no effect on pigmentation in a defined genetic background. By contrast, Cui *et al*.[42] report that p53 mutant mice show a relatively pale skin color. From this perspective, *Trp53* is perhaps a 'better' candidate gene for pigmentary variation than *Pomc*; indeed, Beckman and colleagues[44,45] have suggested previously that clinal variation in *TP53* haplotypes underlies climatic adaptation in humans. Thus, the same selective pressures responsible for defense against the damaging effects of UV radiation may also contribute to basal differences in pigmentary phenotype.

Although p53 is poised to respond to stress signals in many different cell types, our results suggest that variation in the type of response accounts for both the tissue-specificity and the pleiotropy associated with reduced ribosomal protein dosage, with increased expression of *Kitl* in keratinocytes causing dark skin, and cell cycle arrest and/or apoptosis in the bone marrow causing red cell aplasia (**Fig. 7**). Even reduced body size in $Rps19^{Dsk3}$ mutant mice was rescued by p53 deficiency; thus, most if not all the consequences of hemizygosity for ribosomal protein genes may be due to activation of p53-dependent pathways. In *Drosophila* Minute mutants, a reduced rate of development and altered body size has long been ascribed to a general impairment of cellular protein synthesis[2,13,46]; however, our results suggest an alternative and easily testable explanation that involves activation of *Dmp53*, which encodes the *Drosophila* homolog of p53.

In some respects, the erythroid defect we observed in *Dsk3* mutant mice, albeit mild, is surprising, given previous work[47,48] on animals carrying an *Rps19* targeted allele that show no erythroid abnormalities. However, this study[47,48] found that the nontargeted *Rps19* allele in their model showed compensatory upregulation, which is quite unusual and apparently not the case for the *Dsk3* mutation. This suggests that mice carrying additional, and perhaps multiple, missense alleles of *Rps* genes may show severe erythroid defects, providing an additional model for the human condition. Regardless, tissue-specific variation in the activation of, or response to, p53, is a plausible mechanism to account for Diamond-

Blackfan syndrome in humans, and suggests new avenues for both diagnosis and treatment. For example, efforts to identify mutations in the ~ 75% of affected individuals that do not have mutations in *RPS19* could be expanded beyond ribosomal protein subunit genes to include components of the p53 pathway, and pharmacologic approaches titrated to control p53 activation, expression or downstream effectors in bone marrow may prove to be helpful for treating individuals with red cell aplasia or other bone marrow failure syndromes.

Of the 15 Dsk mutants identified in the original screen[16], 5 were associated with epidermal melanocytosis; the 3 that have yet to be identified and characterized (*Dsk6*, *Dsk8* and *Dsk11*) are very similar to each other and to *Dsk3* and *Dsk4*. These and other additional dark skin mutants may provide a sensitive means to learn more about the control and targets of p53 in an organismal context.

METHODS

Animals and animal experiments

We obtained mice carrying *Kit*^{Wv} from The Jackson Laboratory, *Dct-lacZ* from M. Shin (Fox Chase Cancer Center) and I. Jackson (MRC Human Genetics Unit), *Rps6*^{lox} from G. Thomas (University of Cincinnati)[11], *Tg.K5Cre* from S. Artandi (Stanford University) and J. Jorcano (Epithelial Biomedicine Division CIEMAT)[24] and *Trp53*^{KO} from T. Jacks (Massachusetts Institute of Technology)[37].

For the studies of Kit signaling (**Fig. 4**), we injected P2 animals intraperitoneally with PBS or 25 μg of monoclonal rat antibody to mouse cKit (ACK2, Chemicon). We obtained measurements of hematologic parameters at 8 weeks of age from retroorbital blood samples. For the studies of hematopoietic apoptosis, we flushed bone marrow from femurs of 8-week-old animals with RPMI containing 10% FCS, and we stained thin-layer cell preparations from a cytocentrifuge with Wright-Giemsa. Lineage-negative, cKit-positive bone marrow progenitor cells were identified and analyzed by immunostaining and FACS analysis for cKit, Gr-1, Mac-1, CD-3, CD-4, CD-8, B220 and TER-119 as previously described[39]. We used annexin V-FITC staining (CalBiochem) as a marker for apoptotic cells. Three animals of each genotype were analyzed. All experiments were carried out under a protocol approved by the Stanford Administrative Panel on Laboratory Animal Care.

Genetics

Generation of *Dsk3*/+ and *Dsk4*/+ mice on an isogenic C3HeB/FeJ background[15] and preliminary linkage studies were described previously[16]. For high-resolution mapping, (C3H3B/FeJ – *Dsk* × CAST/Ei)BC_1 backcross progeny were generated and screened as described[17], using SSLP and/or SSCP markers as indicated (**Fig. 2a** and **Supplementary Fig. 2a**). Physical distances and coordinates reflect the mm8 assembly as presented by the UCSC genome browser[49]. All mutations were confirmed with sequencing or restriction digestion of PCR amplicons. For *Dsk3*, markers M1, M2, M7 and M23 represent single-strand conformation polymorphisms apparent from amplicons corresponding, respectively, to 7:24,200,000–24,200,100, 7:25,300,000–25,300,100, 7:24,300,000–24,300,100 and 7:24,900,000–24,900,100.

Rps19^{Dsk3} and *Rps20*^{Dsk4} were genotyped by direct sequencing (*Dsk3*) or by MspI digestion (*Dsk4*) of PCR-amplified genomic DNA. The *Kit*$^{W\text{-}v}$ (ref. 18), *Rps6*^{lox} (ref. 33), *Tg.K5Cre*[24], *Tg.MitfCre*[25], *Trp53*^{KO} (ref. 37) and *Trp53*^{QS} (ref. 36) mutations were genotyped as described previously.

Histology

Tissues for histology were prepared as previously described[16], as were morphometric measurements of skin darkness and Xgal-positive cells[17]. For LacZ staining of embryonic and adult tissues, E15.5 embryos, adult footpads and adult tails were fixed in 4% paraformaldehyde and immersed in X-gal overnight at room temperature. Immunofluorescence for p53 was carried out with rabbit anti-p53 antisera (Novocastra Laboratories) after antigen retrieval using 0.01M citrate buffer, pH 6 in a pressure cooker. We carried out dermal–epidermal separations by immersing tissues in 2 M NaBr at 37 °C. All photomicrographs are representative of at least three animals of each genotype.

Gene expression and statistics

RNA for qRT-PCR and expression array experiments was isolated from the footpad epidermis using Trizol (Invitrogen) and purified using RNeasy (Qiagen). We pooled multiple (2–4) footpads for each replicate and used at least three replicates for each genotype and/or time point. For qRT-PCR, we treated 1 μg of RNA with DNaseI before reverse transcription with Superscript III (Invitrogen). Diluted cDNA (fivefold) was amplified using the LightCycler FastStart DNA Master Plus SYBR Green I System (Roche). Primer sequences for *Kitl*, *Pomc*, *Edn1* and *Gapdh* are available on request.

We used the Illumina Sentrix system (MouseRef-8, BD-26–201) for gene expression profiling, as previously described[50]. Differentially expressed genes were ranked according to a *t* statistic, with associated *P* values corrected for multiple testing according to Benjamini and Hochman[29]. Statistical analyses of physiological and histological phenotypes were carried out with either a two-sample *t*-test, or with multiple regression in which sex and litter were factors, as appropriate.

Supplementary Material

Refer to Web version on PubMed Central for supplementary material.

Acknowledgments

We thank G. Thomas (University of Cincinnati) and S. Volarevic (University of Cincinnati) for *Rps6*^{lox} mice, I. Jackson (MRC Human Genetics Unit) and M. Shin (Fox Chase Cancer Center) for *Dct-lacZ* mice, S. Artandi (Stanford University) and J. Jorcano (Epithelial Biomedicine Division CIEMAT) for *Tg.K5Cre* mice, A. Alizadeh (Stanford University) for *Tg.MitfCre* mice and T. Jacks (Massachusetts Institute of Technology) for *Trp53*^{KO} mice. We thank P. Khavari and U. Francke for their careful review of the work, H. Manuel for technical support and B. Glader for advice regarding Diamond-Blackfan anemia. K.A.M. and C.Y.P. are supported by Mentored Clinical Scientist Development Investigator Awards from the National Institutes of Health. G.S.B. is supported by a Research Project Grant from the National Institutes of Health. Part of this work was supported by a grant from the German Human Genome Project (DHGP) and the National Genome Research Network (NGFN 01GR0430) to M.H.d.A.

References

1. Schultz J. The Minute reaction in the development of Drosophila melanogaster. Genetics. 1929; 14:366–419. [PubMed: 17246581]
2. Lambertsson A. The minute genes in Drosophila and their molecular functions. Adv. Genet. 1998; 38:69–134. [PubMed: 9677706]
3. Oliver ER, Saunders TL, Tarle SA, Glaser T. Ribosomal protein L24 defect in belly spot and tail (Bst), a mouse Minute. Development. 2004; 131:3907–3920. [PubMed: 15289434]
4. Draptchinskaia N, et al. The gene encoding ribosomal protein S19 is mutated in Diamond-Blackfan anaemia. Nat. Genet. 1999; 21:169–175. [PubMed: 9988267]
5. Cmejla R, Cmejlova J, Handrkova H, Petrak J, Pospisilova D. Ribosomal protein S17 gene (RPS17) is mutated in Diamond-Blackfan anemia. Hum. Mutat. 2007; 28:1178–1182. [PubMed: 17647292]

6. Gazda HT, et al. Ribosomal protein S24 gene is mutated in Diamond-Blackfan anemia. Am. J. Hum. Genet. 2006; 79:1110–1118. [PubMed: 17186470]
7. Ellis SR, Lipton JM. Diamond blackfan anemia: a disorder of red blood cell development. Curr. Top. Dev. Biol. 2008; 82:217–241. [PubMed: 18282522]
8. Gazda HT, Sieff CA. Recent insights into the pathogenesis of Diamond-Blackfan anaemia. Br. J. Haematol. 2006; 135:149–157. [PubMed: 16942586]
9. Flygare J, Karlsson S. Diamond-Blackfan anemia: erythropoiesis lost in translation. Blood. 2007; 109:3152–3154. [PubMed: 17164339]
10. Leger-Silvestre I, et al. Specific role for yeast homologs of the Diamond Blackfan anemia-associated Rps19 protein in ribosome synthesis. J. Biol. Chem. 2005; 280:38177–38185. [PubMed: 16159874]
11. Volarevic S, et al. Proliferation, but not growth, blocked by conditional deletion of 40S ribosomal protein S6. Science. 2000; 288:2045–2047. [PubMed: 10856218]
12. Angelini M, et al. Missense mutations associated with Diamond-Blackfan anemia affect the assembly of ribosomal protein S19 into the ribosome. Hum. Mol. Genet. 2007; 16:1720–1727. [PubMed: 17517689]
13. Morata G, Ripoll P. Minutes: mutants of Drosophila autonomously affecting cell division rate. Dev. Biol. 1975; 42:211–221. [PubMed: 1116643]
14. Vousden KH, Lane DP. p53 in health and disease. Nat. Rev. Mol. Cell Biol. 2007; 8:275–283. [PubMed: 17380161]
15. Hrabe de Angelis MH, et al. Genome-wide, large-scale production of mutant mice by ENU mutagenesis. Nat. Genet. 2000; 25:444–447. [PubMed: 10932192]
16. Fitch KR, et al. Genetics of dark skin in mice. Genes Dev. 2003; 17:214–228. [PubMed: 12533510]
17. Van Raamsdonk CD, Fitch KR, Fuchs H, de Angelis MH, Barsh GS. Effects of G-protein mutations on skin color. Nat. Genet. 2004; 36:961–968. [PubMed: 15322542]
18. Mackenzie MA, Jordan SA, Budd PS, Jackson IJ. Activation of the receptor tyrosine kinase Kit is required for the proliferation of melanoblasts in the mouse embryo. Dev. Biol. 1997; 192:99–107. [PubMed: 9405100]
19. Hirobe T. Histochemical survey of the distribution of the epidermal melanoblasts and melanocytes in the mouse during fetal and postnatal periods. Anat. Rec. 1984; 208:589–594. [PubMed: 6731864]
20. Mayer TC. The migratory pathway of neural crest cells into the skin of mouse embryos. Dev. Biol. 1973; 34:39–46. [PubMed: 4595498]
21. Cable J, Jackson IJ, Steel KP. Mutations at the W locus affect survival of neural crest-derived melanocytes in the mouse. Mech. Dev. 1995; 50:139–150. [PubMed: 7619726]
22. Steel KP, Davidson DR, Jackson IJ. TRP-2/DT, a new early melanoblast marker, shows that steel growth factor (c-kit ligand) is a survival factor. Development. 1992; 115:1111–1119. [PubMed: 1280558]
23. Fromont-Racine M, Senger B, Saveanu C, Fasiolo F. Ribosome assembly in eukaryotes. Gene. 2003; 313:17–42. [PubMed: 12957375]
24. Ramirez A, et al. A keratin K5Cre transgenic line appropriate for tissue-specific or generalized Cre-mediated recombination. Genesis. 2004; 39:52–57. [PubMed: 15124227]
25. Alizadeh A, Fitch KR, Niswender CM, McKnight GS, Barsh GS. Melanocytelineage expression of Cre recombinase using Mitf regulatory elements. Pigment Cell Melonoma Res. 2008; 21:63–69.
26. Hirobe T. Role of keratinocyte-derived factors involved in regulating the proliferation and differentiation of mammalian epidermal melanocytes. Pigment Cell Res. 2005; 18:2–12. [PubMed: 15649147]
27. Kunisada T, et al. Transgene expression of steel factor in the basal layer of epidermis promotes survival, proliferation, differentiation and migration of melanocyte precursors. Development. 1998; 125:2915–2923. [PubMed: 9655813]

28. Nishikawa S, et al. In utero manipulation of coat color formation by a monoclonal antic-kit antibody: two distinct waves of c-kit-dependency during melanocyte development. EMBO J. 1991; 10:2111–2118. [PubMed: 1712289]
29. Benjamini Y, Hochberg Y. Controlling the false discovery rate: a practical and powerful approach to multiple testing. J. Roy. Statist. Soc. Ser. B. Methodological. 1995; 57:289–300.
30. Ellisen LW, et al. REDD1, a developmentally regulated transcriptional target of p63 and p53, links p63 to regulation of reactive oxygen species. Mol. Cell. 2002; 10:995–1005. [PubMed: 12453409]
31. Barak Y, Juven T, Haffner R, Oren M. mdm2 expression is induced by wild type p53 activity. EMBO J. 1993; 12:461–468. [PubMed: 8440237]
32. Panic L, et al. Ribosomal protein S6 gene haploinsufficiency is associated with activation of a p53-dependent checkpoint during gastrulation. Mol. Cell. Biol. 2006; 26:8880–8891. [PubMed: 17000767]
33. Sulic S, et al. Inactivation of S6 ribosomal protein gene in T lymphocytes activates a p53-dependent checkpoint response. Genes Dev. 2005; 19:3070–3082. [PubMed: 16357222]
34. Loonstra A, et al. Growth inhibition and DNA damage induced by Cre recombinase in mammalian cells. Proc. Natl. Acad. Sci. USA. 2001; 98:9209–9214. [PubMed: 11481484]
35. Chan EL, et al. Homozygous K5Cre transgenic mice have wavy hair and accelerated malignant progression in a murine model of skin carcinogenesis. Mol. Carcinog. 2007; 46:49–59. [PubMed: 17013830]
36. Johnson TM, Hammond EM, Giaccia A, Attardi LD. The p53QS transactivation-deficient mutant shows stress-specific apoptotic activity and induces embryonic lethality. Nat. Genet. 2005; 37:145–152. [PubMed: 15654339]
37. Jacks T, et al. Tumor spectrum analysis in p53-mutant mice. Curr. Biol. 1994; 4:1–7. [PubMed: 7922305]
38. Miyake K, et al. RPS19 deficiency leads to reduced proliferation and increased apoptosis but does not affect terminal erythroid differentiation in a cell line model of Diamond-Blackfan anemia. Stem Cells. 2008; 26:323–329. [PubMed: 17962699]
39. Rossi DJ, et al. Deficiencies in DNA damage repair limit the function of haematopoietic stem cells with age. Nature. 2007; 447:725–729. [PubMed: 17554309]
40. Amsterdam A, et al. Many ribosomal protein genes are cancer genes in zebrafish. PLoS Biol. 2004; 2:e139. [PubMed: 15138505]
41. McCulloch EA, Siminovitch L, Till JE, Russell ES, Bernstein SE. The cellular basis of the genetically determined hemopoietic defect in anemic mice of genotype Sl-Sld. Blood. 1965; 26:399–410. [PubMed: 5317869]
42. Cui R, et al. Central role of p53 in the suntan response and pathologic hyperpigmentation. Cell. 2007; 128:853–864. [PubMed: 17350573]
43. Slominski A, et al. Preservation of eumelanin hair pigmentation in proopiomelanocortin-deficient mice on a nonagouti (a/a) genetic background. Endocrinology. 2005; 146:1245–1253. [PubMed: 15564334]
44. Sjalander A, Birgander R, Kivela A, Beckman G. p53 polymorphisms and haplotypes in different ethnic groups. Hum. Hered. 1995; 45:144–149. [PubMed: 7615299]
45. Beckman G, et al. Is p53 polymorphism maintained by natural selection? Hum. Hered. 1994; 44:266–270.
46. Marygold SJ, et al. The ribosomal protein genes and Minute loci of Drosophila melanogaster. Genome Biol. 2007; 8:R216. [PubMed: 17927810]
47. Matsson H, et al. Erythropoiesis in the Rps19 disrupted mouse: analysis of erythropoietin response and biochemical markers for Diamond-Blackfan anemia. Blood Cells Mol. Dis. 2006; 36:259–264. [PubMed: 16458028]
48. Matsson H, et al. Targeted disruption of the ribosomal protein S19 gene is lethal prior to implantation. Mol. Cell. Biol. 2004; 24:4032–4037. [PubMed: 15082795]
49. Karolchik D, et al. The UCSC Genome Browser Database. Nucleic Acids Res. 2003; 31:51–54. [PubMed: 12519945]

50. Strehlow AN, Li JZ, Myers RM. Wild-type huntingtin participates in protein trafficking between the Golgi and the extracellular space. Hum. Mol. Genet. 2007; 16:391–409. [PubMed: 17189290]

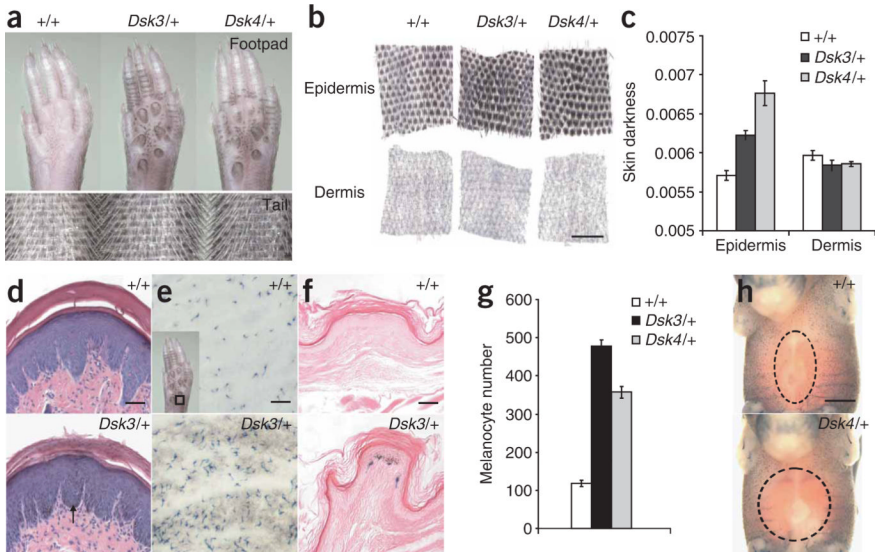

Figure 1.

Dsk3 and *Dsk4* pigmentary phenotype. (**a,b**) Whole footpads and tails (**a**) or separated tail epidermis and dermis (**b**) from adult animals. (**c**) Skin darkness (mean ± s.e.m.) of epidermis and dermis for each genotype. (**d**) Histological sections of footpad epidermis show pigment accumulation in the epidermis (arrow). (**e–h**) Xgal-stained adult footpad epidermis (**e**, inset), whole footpad (**f**) and E15.5 embryos (**h**) from +/+ and *Dsk4*/+ animals that also carry the *Dct-lacZ* transgene. A dashed circle denotes the area without Xgal-positive cells. (**g**) Number of Xgal-positive cells (mean ± s.e.m.) from the location shown in **e** (inset). For **c** and **g**, *P* values for mutant versus control (based on a two-tail *t*-test) are 1.53×10^{-5} and 0.0036 (**c**), and 0.0017 and 0.0036 (**g**), for *Dsk3*/+ and *Dsk4*/+, respectively. Scale bars: **b**, 500 μm; **d,f**, 50 μm; **e,h**, 300 μm.

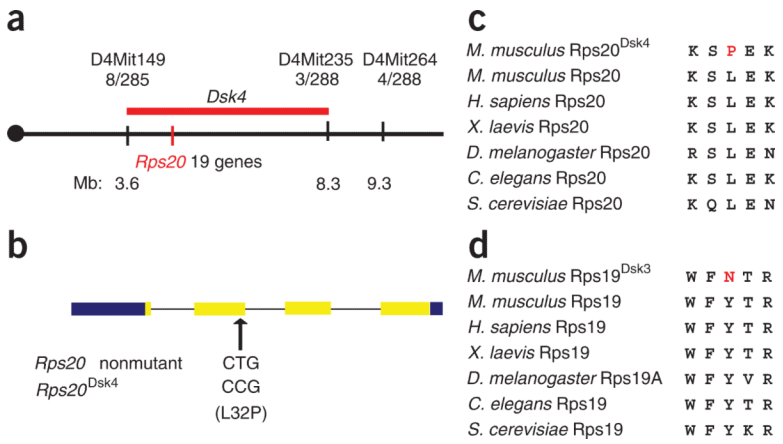

Figure 2.

Positional cloning of *Dsk* mutations. (**a**) Genetic and physical maps of the *Dsk4* critical interval on mouse chromosome 4. Recombination frequencies (stated as the number of recombinant chromosomes between the marker and *Dsk3*, over the number of informative chromosomes evaluated) are given immediately below each marker. Approximate physical coordinates in megabases (Mb) are given below. (**b**) The position and sequence of the *Dsk4* point mutation is shown relative to the exon–intron structure of *Rps20* where untranslated and protein-coding regions are represented by blue and yellow, respectively. (**c,d**) Predicted protein sequences for $Rps20^{Dsk4}$ (**c**) and $Rps19^{Dsk3}$ (**d**), aligned with homologous sequence in other species.

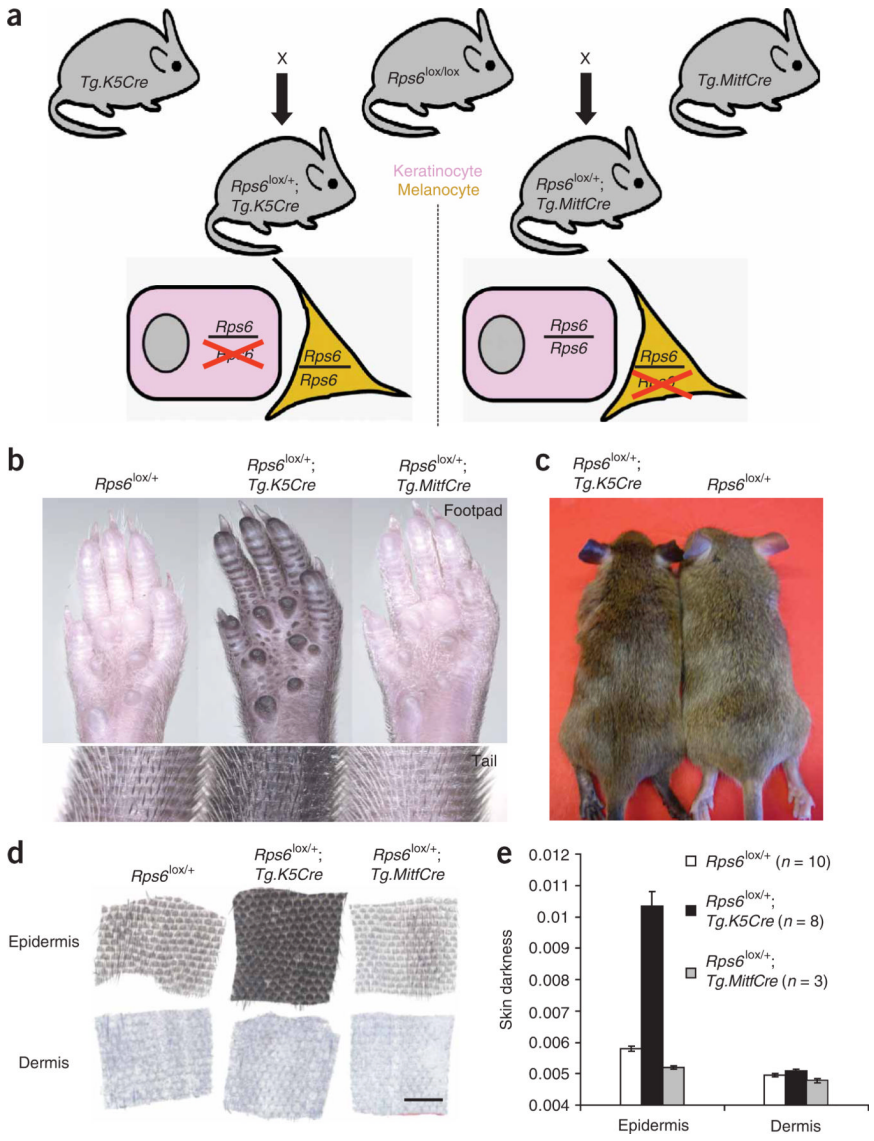

Figure 3.

Tissue-specific modulation of *Rps6* gene dosage. (**a**) One copy of *Rps6* was removed either from keratinocytes (pink, using *Tg.K5Cre*) or from melanocytes (yellow, using *Tg.MitfCre*). (**b–d**) Whole footpads and tails (**b**), ears (**c**) and separated tail epidermis and dermis (**d**) from animals of the indicated genotype. (**e**) Skin darkness (mean ± s.e.m.); *P* values for mutant versus control (based on a two-tail *t*-test) are 1.7×10^{-5} and 6.7×10^{-5} for keratinocyte (*Tg.K5Cre*)- and melanocyte (*Tg.MitfCre*)-specific *Rps6*, respectively. Scale bar in **d**, 500 μm.

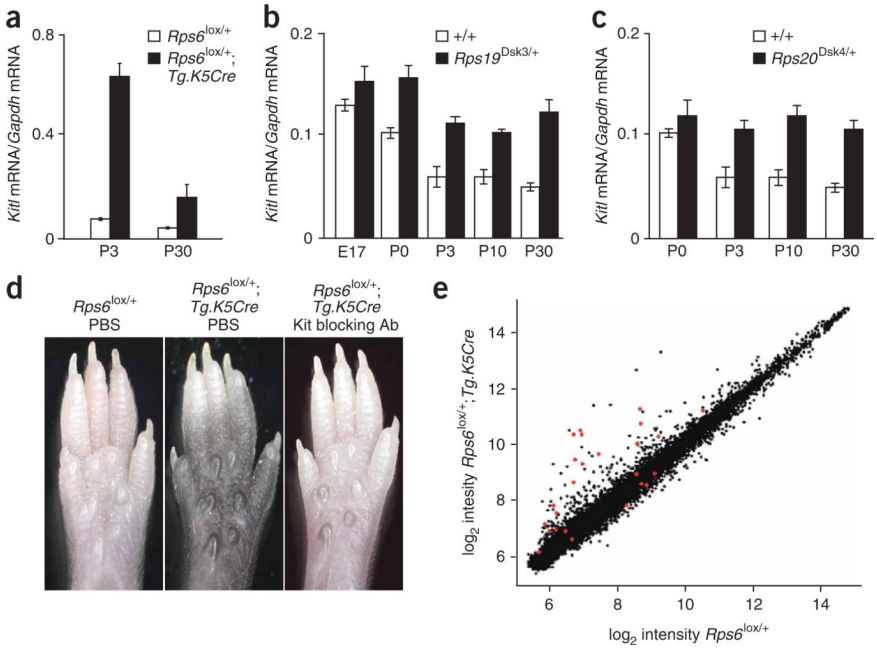

Figure 4.

Gene expression and Kit signaling in *Rps* mutants. (**a–c**) Expression of *Kitl* mRNA in footpad epidermis relative to *Gapdh* mRNA (mean ± s.e.m.) in animals of the indicated genotype at different times. Mutant versus control *P* values (two-tail) are *Rps6* P3 $P = 0.002$, P30 $P = 0.003$; $Rps19^{Dsk3/+}$ P0 $P = 0.039$, P3 $P = 0.007$, P10 $P = 0.005$, P30 $P = 0.0004$; $Rps20^{Dsk4/+}$ P3 $P = 0.017$, P10 $P = 0.036$, P30 $P = 0.038$ ($n = 3–4$ for each assay). (**d**) Appearance of P8 whole footpads from animals of the indicated genotype 6 days after intraperitoneal injection with PBS or Kit blocking antisera. Representative results are shown for each genotype and treatment condition ($n = 4–6$ for each class). (**e**) Microarray results for keratinocyte-specific *Rps6* versus control footpad epidermis for each of 24,611 transcripts represented on the array. Each dot represents the mean for three mutant ($Rps6^{lox/+}$;*Tg.K5Cre*/+) and three control ($Rps6^{lox/+}$) samples; transcripts associated with *P* values ≤0.05 (after multiple testing correction) are indicated in red and identified in **Supplementary Table 1**.

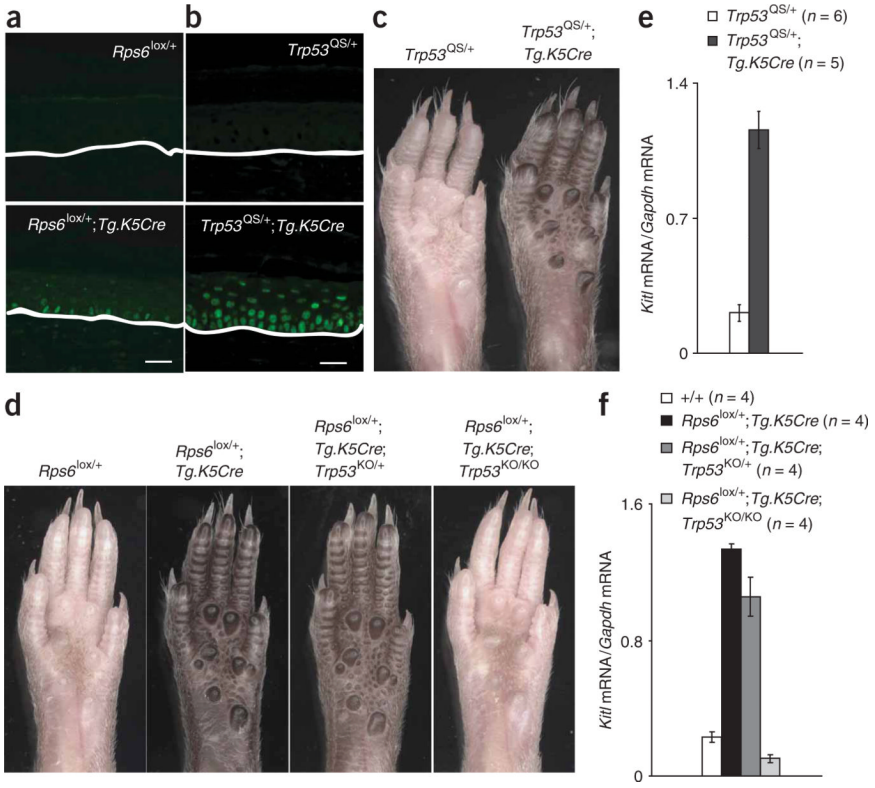

Figure 5.

p53 is sufficient and necessary to induce dark skin. (**a,b**) Immunofluorescence for p53 in footpad sections; white lines mark the dermal-epidermal junction. (**c,d**) Whole footpads from adult animals; all results shown are representative of at least three animals for each genotype. (**e,f**) Expression of *Kitl* mRNA in P30 footpad epidermis relative to *Gapdh* mRNA (mean ± s.e.m.) in animals of the indicated genotypes (two-tail *P* values are $Trp53^{QS/+}$ versus $Trp53^{QS/+}$; *Tg.K5Cre*/+ $P = 0.00016$; $Rps6^{+/+}$ vs. $Rps6^{lox/+}$; *Tg.K5Cre* $P = 5 \times 10^{-7}$; $Rps6^{lox/+}$; *Tg.K5Cre* vs. $Rps6^{lox/+}$; *Tg.K5Cre*; $Trp53^{KO/KO}$ $P = 3.2 \times 10^{-7}$). Scale bars: **a,b**, 25 μm.

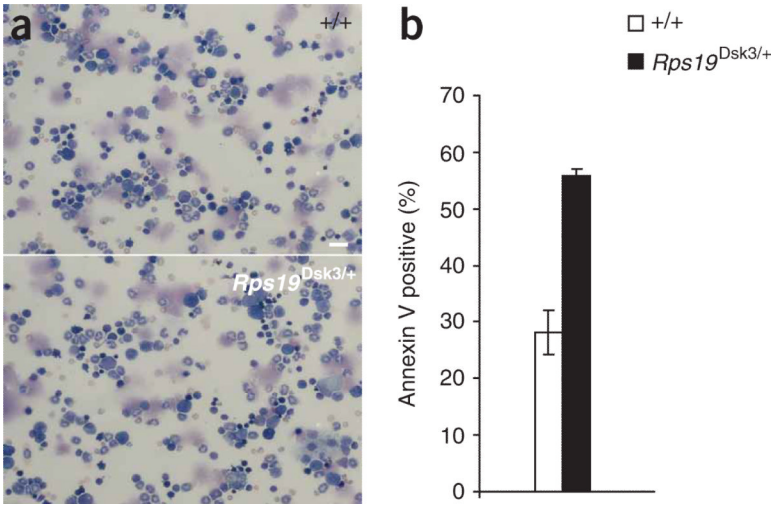

Figure 6.

Effect of *Rps19*^{Dsk3} on bone marrow. (**a**) Representative photomicrographs of bone marrow aspirates (stained with Wright-Giemsa) from animals of the indicated genotypes. Scale bar, 40 μm. (**b**) The number of annexin V–positive bone marrow progenitor cells (lineage-cKit+) in nonmutant and *Rps19*$^{Dsk3/+}$ animals (± s.e.m.) at 8 weeks of age; $n = 3$ for each genotype. *Rps19*$^{Dsk3/+}$ differed significantly from *Rps19*$^{+/+}$ ($P = 0.013$ based on a two-tail *t*-test).

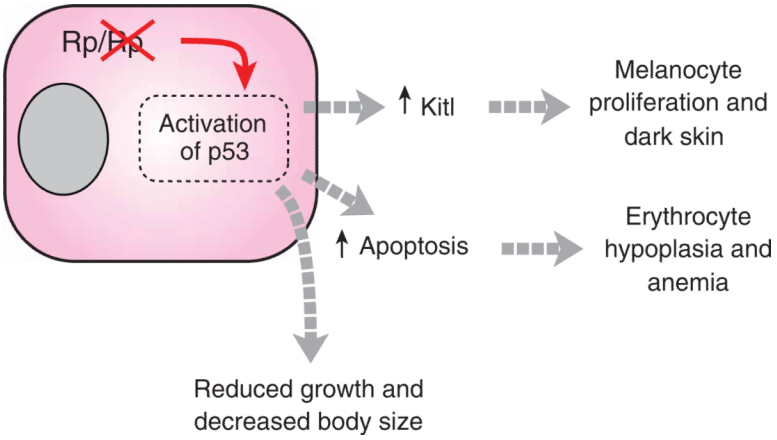

Figure 7.

Pathophysiology of mutations affecting ribosomal proteins (Rp). As described in the text, reduced dosage of *Rps6*, *Rps19* or *Rps20* triggers stabilization and/or activation of p53, which gives rise to a pleiotropic phenotype whose components depend on the sensitivity and response of individual cell types and on specific downstream targets of p53. All of the phenotypes can be rescued by deficiency for *Trp53*.

Table 1

Effects of *Rps19* and *Trp53* mutations on erythrocytes and body weight

	Inbred (C3HeB/FeJ)		Mixed			
Trp53 genotype	+/+	+/+	+/+	+/+	KO/+	KO/KO
Rps19 genotype	+/+	*Dsk3*/+	+/+	*Dsk3*/+	*Dsk3*/+	*Dsk3*/+
No. of animals (male:female)	5 (3:2)	6 (2:4)	14 (7:7)	16 (9:7)	21 (11:10)	8 (4:4)
RBC	9.35 ± 0.16	8.67 ± 0.17 (P = 0.02)[a]	9.81 ± 0.11	9.07 ± 0.10 (P = 0.00004)[b]	9.68 ± 0.08 (P = 0.00001)[c]	9.83 ± 0.17 (P = 0.0012)[d]
MCV	50.9 ± 0.22	51.6 ± 0.20 (P = 0.04)[a]	48.9 ± 0.28	49.8 ± 0.26 (P = 0.03)[b]	48.8 ± 0.22 (P = 0.004)[c]	49.0 ± 0.38
Reticulocytes	702 ± 43	297 ± 40 (P = 0.0002)[a]	n.d.	n.d.	n.d.	n.d.
No. of animals (male:female)	10 (2:8)	13 (7:6)	3 (2:1)	6 (4:2)	9 (5:4)	
Weight (g)	11.3 ± 0.23	9.54 ± 0.18 (P = 1.7 × 10^{-6})[a]	13.6 ± 0.52	11.1 ± 0.35 (P = 0.007)[b]	12.6 ± 0.28 (P = 0.003)[c]	n.d.

Blood counts were obtained at 8 weeks of age; body weight was obtained at P21. All values are given as mean ± s.e.m. (with P values based on multiple regression in which litter and sex are factors); different cohorts of animals were used for the hematological and the weight studies.

RBC, red blood cellcount; MCV, mean corpuscular volume; n.d., not done.

[a] *Rps19*$^{+/+}$ versus *Rps19*$^{Dsk3/+}$ on inbred background.

[b] *Rps19*$^{+/+}$ versus *Rps19*$^{Dsk3/+}$ on mixed background.

[c] *Rps19*$^{Dsk3/+}$ versus *Rps19*$^{Dsk3/+}$; *Trp53*$^{KO/+}$.

[d] *Rps19*$^{Dsk3/+}$ versus *Rps19*$^{Dsk3/+}$; *Trp53*$^{KO/KO}$.